

# Composition Dependence of the Grain size, Activation Energy and Coordination Number in $\text{Ge}_{40-x}\text{In}_x\text{Se}_{60}$ ( $10 \leq x \leq 40$ at.%) Thin Films

El -Sayed M. Farag<sup>(1)</sup> and M. M. Sallam<sup>(2)</sup>

<sup>(1)</sup> Basic Science of Engineering Dept., Faculty of Engineering, Shebin El-Kom, Minufiya University, Egypt.

<sup>(2)</sup> Physics Dept., Faculty of Science, Ain Shams University, Cairo, Egypt.

Bulk glasses with chemical composition of  $\text{Ge}_{40-x}\text{In}_x\text{Se}_{60}$  ( $10 \leq x \leq 40$  at.%) are prepared from high purity constituent elements. Vacuum thermal evaporation technique is used to deposit thin films of these materials on glass substrates. After annealing at 485K for 4hs. the crystalline nature of the prepared thin films are investigated by X-ray diffraction (XRD). The analysis of the X-ray measurements indicates the existence of two crystalline phases namely  $\text{GeInSe}$  and  $\text{In-Se}$  phases. Electrical conductivity is measured in vacuum, in temperature range 300-430K of the as-deposit and annealed films for the studied compositions. The electrical conductivity exhibits two types of conduction mechanisms, the first mechanism due to hopping is applicable from 300-333K while the free carrier describes the conductivity in the temperature range from 333-430K. The annealed films show more conductivity and less activation energy than the as-deposited films this is due to the crystalline nature of the annealed films. Increasing In content increases the grain size and the coordination number while the activation energy is decreased.

## 1. Introduction:

Amorphous semiconductor chalcogenides have recently gained considerable attention due to their interesting optical properties and technological applications. Their promising material science applications include photo-structural optical recording [1,2], advanced IR optical fiber [3], and acoustic-optic devices [4,5]. Such wide-ranging applications are possible due to some unique phenomena like photo-induced structural transformations [6].

The Ge-Se-In ternary is a prototypical chalcogenide system and forms bulk glasses over a large range of compositions extending up to 15 at % In and up to 60-90 at % Se, with the remainder being Ge [7]. Thus, it is possible to scan with one glassy family a very wide range of covalent coordination number,  $Z$ . This system is, therefore, ideal for the analysis of the variation of a given physical property with  $Z$ . However, the calculation of the key parameter,  $Z$ , requires the knowledge of the coordination numbers (CN) of all the constituents of the alloy. For the system under investigation, the CN(Ge) and CN(Se) respect the Mott "8N" rule [8], where N is the number of outer shell electrons. Nevertheless, the CN(In) is a subject of great controversy where coordinations equal to 1 [9,10], 3 [11,12], 4 [13-15], and 5 [16] have been proposed. Given the diversity of these values and in an attempt to resolve the controversy regarding the CN(In) in this system and to be able to calculate  $Z$  for the investigated compositions.

In the current work, we report and discuss the composition dependence of the grain size, coordination number and activation energy of conduction in  $\text{Ge}_{40-x}\text{In}_x\text{Se}_{60}$  ( $10 \leq x \leq 40$  at.%) thin films.

## 2. Experimental:

The  $\text{Ge}_{40-x}\text{In}_x\text{Se}_{60}$  ( $10 \leq x \leq 40$  at.%) bulk materials have been prepared according to the well established melt-quench technique. Appropriate atomic percentages of high purity elements (5N) are vacuum sealed ( $10^{-5}$  Torr) into fused silica tubes of length 80 mm and internal diameter 8mm. The sealed tubes are then heated in an electric furnace up to 1300 K for 20 h. During the melt process, the ampoules were frequently rocked to intermix the constituents and to increase homogenization of the liquid. After complete melting and homogenization, the tubes are quenched in an ice-water mixture to obtain the glass.

Amorphous Ge-In-Se films are obtained by standard vacuum thermal evaporation of Ge-In-Se bulk glasses. Bulk glass with a composition identical to the one of the film is evaporated from an open tungsten boat onto an ultrasonically cleaned glass substrate (microscope slide). The pressure inside the vacuum chamber is maintained at a value lower than  $10^{-5}$  Torr using a high vacuum coating unit (Edwards E 306A). The substrates are kept at room temperature during the deposition. The source-substance distance is 10 Cm. The films are kept inside the deposition chamber for 24 h to achieve metastable equilibrium. The temperature of the evaporation and the deposition rate were fixed during deposition at pre-determined values to maintain the stoichiometry of the deposited films during film growth. Compositions of the films were analyzed using energy-dispersive X-ray analysis EDAX (JSM 6400 JEOL model SEM attached with NORAN, EDX detector). The films were of different thickness in the range 0.25-0.3  $\mu\text{m}$  thick and have been measured using a

multiple beam interferometer, the error in film thickness values was estimated to be  $\pm 1.5\%$  [17]. X-ray diffraction technique is used to check the structure of the prepared samples. The measurements are performed using filtered Cu  $K_{\alpha}$  radiation (Philips PW 1700) operated at 40 kV and 25 mA. The amorphous  $\text{Ge}_{40-x}\text{In}_x\text{Se}_{60}$  ( $10 \leq x \leq 40$  at.%) films were annealed at 485 K attained with rate 5 K/min then kept constant for 4hs in vacuum  $\cong 10^{-3}$  Torr. The annealed films were checked by X-ray diffraction which shows structure transformation into crystalline phase. DC electrical conductivity measurements were carried out for both virgin and annealed films as a function of temperature in the dark at 300-430K temperature range after vacuum evaporating of gold electrodes at bottom were used for the electrical contact. The co-planar structure (length  $\cong 1.2$  cm and electrode separation  $\cong 2$  mm) was used for the present measurements. The current-voltage measurements showed that the applied contacts were ohmic. All conductivity measurements were done under vacuum ( $\cong 10^{-3}$  Torr) using an Oxford cryostat (type Oxford DN-1714) connected to an Oxford ITC-503 temperature controller of accuracy  $0.01^\circ$ , and a Keithley type E 616 A digital electrometer and the errors in the electrometer readings were  $\pm 0.03\%$ . A calibrated differential scanning calorimeter (Shimadzu-DSC 50), was used to obtain the thermal curve of  $\text{Ge}_{20}\text{In}_{20}\text{Se}_{60}$  as an example.

### 3. Results and Discussion:

#### 3.1. X-ray diffraction:

A DSC trace for  $\text{Ge}_{20}\text{In}_{20}\text{Se}_{60}$  chalcogenide glass as an example in the temperature range from room temperature to complete crystallization is presented in Fig.(1). Two characteristic phenomena are clear in the studied temperature region. The first one ( $T_{g1}$  and  $T_{g2}$ ) corresponds to glass transition temperatures, the second one ( $T_c$ ) corresponds to the onset crystallization temperature, ( $T_p$ ) identifies the crystallization temperature. The appearance of a double glass transition indicates phase separation occurring during the thermal treatment. The phenomenon of double glass transition has been observed in many glassy systems [18, 24, 28, 31].

The X-ray diffraction patterns for the as-deposited and annealed films at 485K for 4hs are examined. Analysis of the X-ray diffraction pattern reveals that the observed crystalline peaks are due to  $\text{GeInSe}$  and  $\text{In}_2\text{Se}_3$  phases as shown in Fig.(2). The grain size of the first phase was calculated from X-ray diffraction pattern using the Debye-Scherrer formula [23, 30].

$$L = 0.9 \lambda / B \cos \theta \quad (1)$$

where L is the grain size in angstroms of the films,  $\lambda$  is the wavelength,  $\theta$  is the diffraction angle and B is the full width at half maximum.

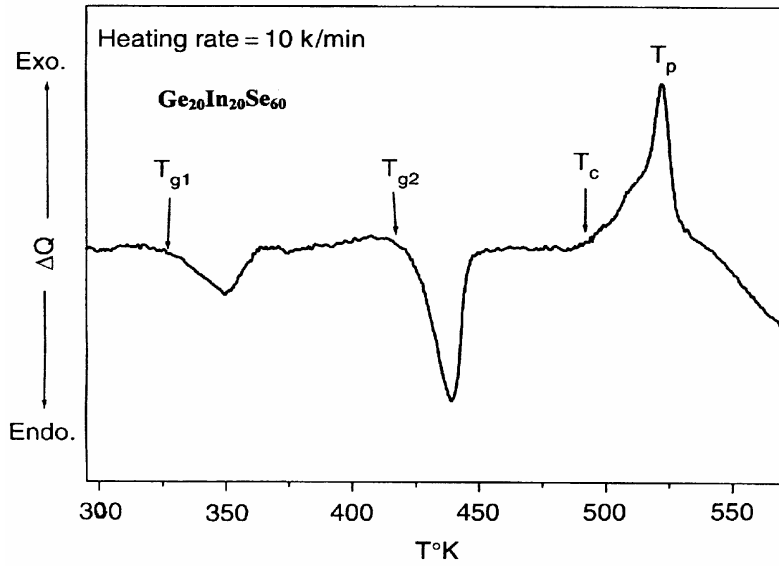


Fig.(1): Typical DSC curve for  $\text{Ge}_{20}\text{In}_{20}\text{Se}_{60}$  glass.

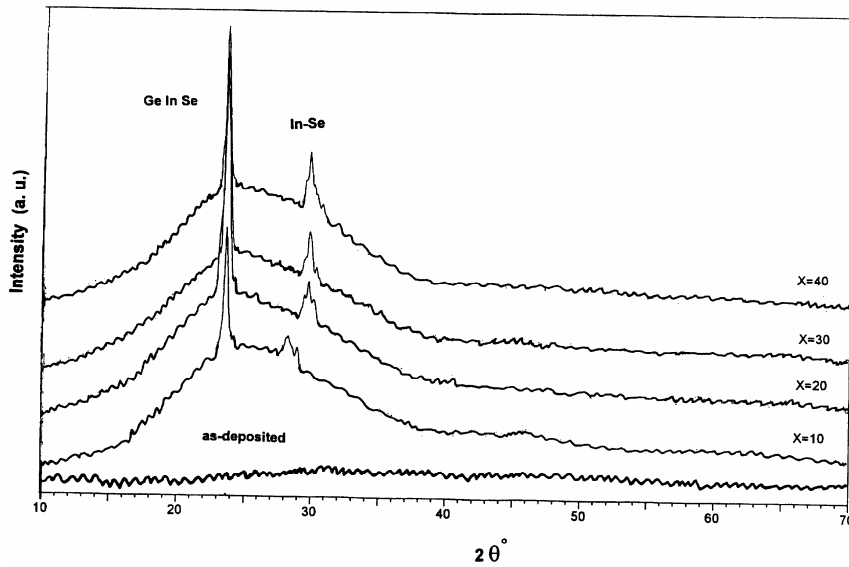


Fig. (2): X-ray diffractogram for the as-deposited and annealed  $\text{Ge}_{40-x}\text{In}_x\text{Se}_{60}$  ( $10 \leq x \leq 40$  at.%) thin films.

### 3.2. Electrical conductivity:

The effect of In content on the electrical conductivity ( $\sigma$ ) of the as-prepared  $\text{Ge}_{40-x}\text{In}_x\text{Se}_{60}$  ( $10 \leq x \leq 40$  at.%) thin films of thickness 0.25-0.3  $\mu\text{m}$  deposited onto glass substrate held during heating from 300-430 K. The dark electrical conductivity ( $\sigma$ ) as a function of reciprocal temperature for as-prepared films is shown in Fig.(3) according to the well known Arrhenius equation:

$$\sigma = \sigma_0 \exp(-\Delta E/kT) \quad (2)$$

where  $\sigma_0$  is the pre-exponential factor ( $\Omega^{-1} \text{cm}^{-1}$ ),  $\Delta E$  is the activation energy (eV) and  $k$  is the Boltzmann constant

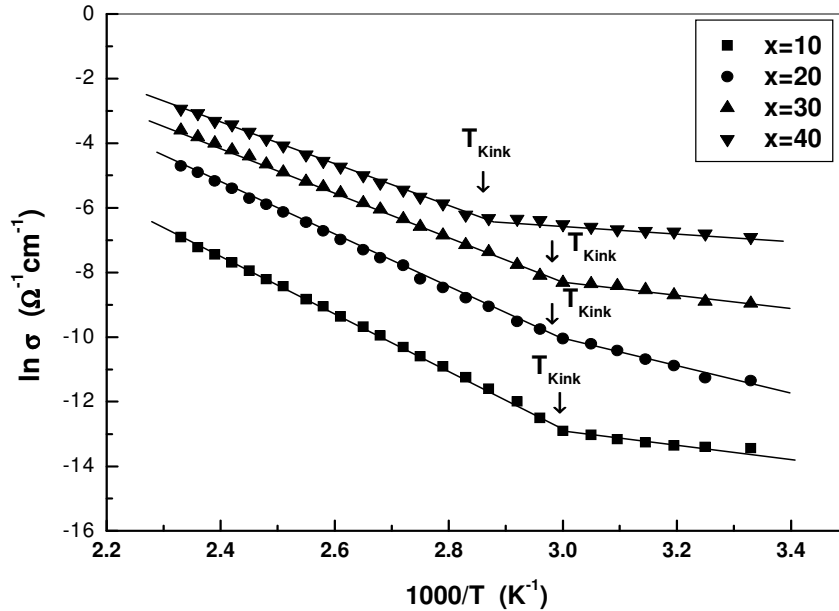


**Fig.(3):** Plot of conductivity versus reciprocal temperature for the as-deposited amorphous  $\text{Ge}_{40-x}\text{In}_x\text{Se}_{60}$  ( $10 \leq x \leq 40$  at.%) thin films.

The electrical results exhibit two types of conduction mechanisms. Below certain temperature, called  $T_{\text{kink}} \approx 300\text{K}$  the electrical conductivity shows a slight decrease with decreasing temperature corresponds to transport by extrinsic or hopping conduction. The presence of a hopping regime strongly suggests localized states as band tail [19]. On the other hand, at temperature  $T > T_{\text{kink}}$  the exponential increase of  $\sigma$  with  $T$  can be regarded as a regular band-

type conduction in extended state which called free carrier conduction. Where the measured conductivity is the sum of two components as:

$$\sigma = \sigma_{\text{hop}} + \sigma_{\text{ext}} \quad (3)$$

Where  $\sigma_{\text{hop}}$  is the contribution of conduction due to hopping between the nearest localized states and  $\sigma_{\text{ext}}$  is the contribution of conduction between the extended states. The position of  $T_{\text{kink}}$  depends on In content, it shifts to higher temperature with increasing In content, can either due to the excitation of the charge carries from a shallow acceptor level or due to the predominance of the hopping conduction mechanism. Excitation of shallow impurity levels is unlikely because the energy levels associated with In vacancies are found to be 30 meV [20].

To study the effect of annealing temperature (485 K for 4 h) on the electrical conductivity of  $\text{Ge}_{40-x}\text{In}_x\text{Se}_{60}$  ( $10 \leq x \leq 40$  at.%) thin films the values of  $\ln\sigma$  vs.  $1/T$  were plotted for the annealed films. The conductivity of annealed films is higher than the as-deposit (virgin) films and the linear plot indicates the semi conducting behavior of the films as shown in Fig.(4). There is a general trend of decrease in activation energy with increase In content while the activation energy of the annealed films is lower than of the virgin films as shown in Fig. (5a). The increase in the electrical conductivity and the decrease in the activation energy for the films after annealing could be attributed to the amorphous-crystalline transformation as explained by Seto's model [21]. A polycrystalline film material contains a large number of micro crystallites with grain boundaries between them. At the grain boundary of each of the crystallites the incomplete atomic bonding can act as trap centers. These trap centers can trap the charge carriers at the grain boundaries, and hence a space charge can be built up locally [22]. The authors Kumar *et al.* [14, 23] have supposed that In induces structural changes in the Ge-Se host network. On the other hand, the decrease of bond energy with increasing In content is responsible for increasing the material's electrical conductivity and decreasing the strength or rigidity of the lattice and consequently the glass softening temperature [24]. Leading, respectively, to a distribution of the charged defect states balance, a shift of the Fermi level and the possibility of new trap states in the mobility gap.

In ternary system, nearest-neighbor coordination obeys the 8N rule, where N is the valence of an atom. Accordingly, the numbers of the nearest-neighbor atoms for Ge, Se and In are, respectively, 4, 2 and 3. Moreover, it should be pointed out that z is an important parameter for describing the glass-forming tendencies topologically [25]. The average coordination number z for

the composition  $\text{Ge}_{40-x}\text{In}_x\text{Se}_{60}$  ( $10 \leq x \leq 40$  at.%) have been calculated by using the relation:

$$z = 4(40-x) + 3x + 2(60) \quad (4)$$

The values of  $z$  in the interval  $2.4 \leq z \leq 2.7$  are concerned with in view of the constraint-counting argument originally proposed by Phillips for amorphous covalent materials [25-27].

The thermal activation energy increases with the calculated values of the average coordination number  $z$  for the glassy alloys  $\text{Ge}_{40-x}\text{In}_x\text{Se}_{60}$  as shown in Fig. (5b). While, the grain size of the films increases with increasing In content as shown in Fig. (6) these results are in good agreement with those obtained by many authors [32, 33]. Assuming that In atoms in these films bond tetrahedrally, it is shown that  $E_F$  moves towards the valence band with change in composition and, hence, these films remain p-type [29]. At low In content ( $x = 10$ ) the peak intensity is very low and lead to formation  $\text{In}_2\text{Se}_3$  clusters [30]. When In content increases, the formation of  $\text{In}_6\text{Se}_7$  phase may be attributed to the interaction of  $\text{In}_2\text{Se}_3$  and escaped Se. Therefore, the peak intensity increases with increasing In content [19].

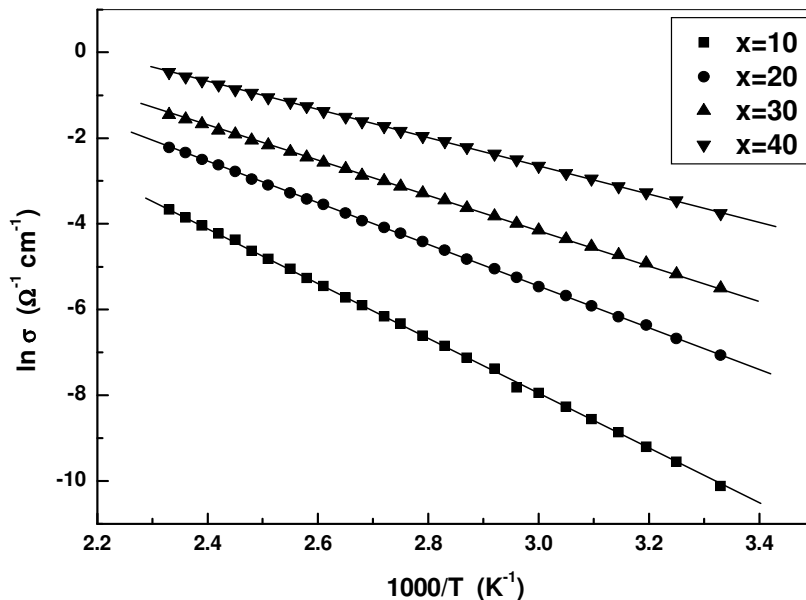


**Fig. (4):** Plot of conductivity versus reciprocal temperature of annealed  $\text{Ge}_{40-x}\text{In}_x\text{Se}_{60}$  ( $10 \leq x \leq 40$  at.%) thin films at 485 K for 4 hs.

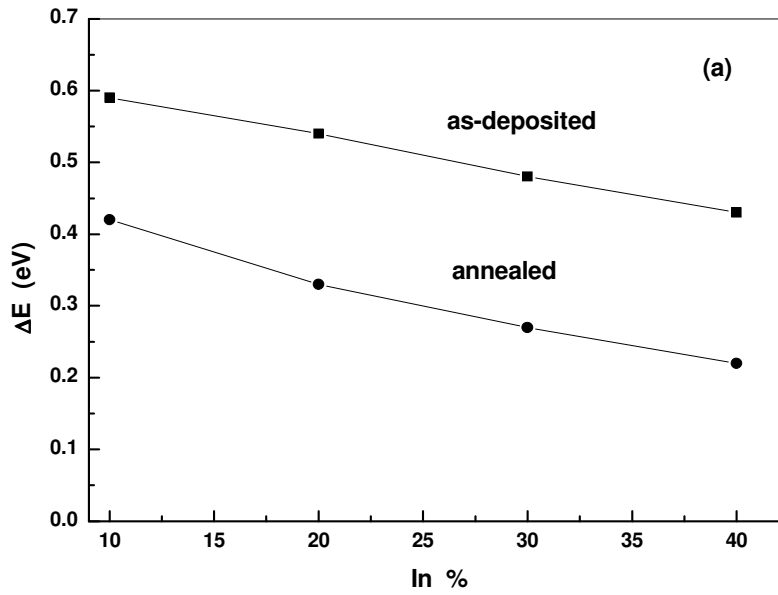


**Fig. (5a):** Variation of activation energy with In content of as-deposited and annealed for  $\text{Ge}_{40-x}\text{In}_x\text{Se}_{60}$  ( $10 \leq x \leq 40$  at.%) thin films.

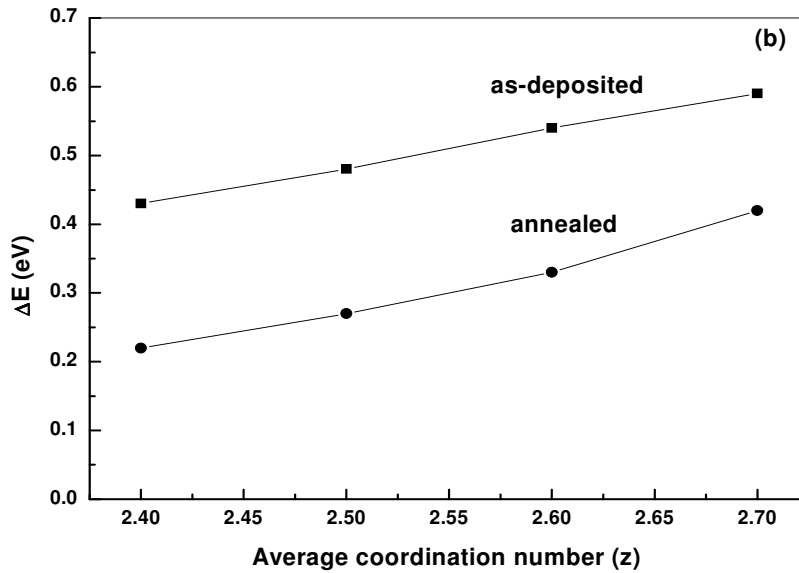


**Fig. (5b):** Variation of the thermal activation energy with the calculated values of the average coordination number  $Z$  for  $\text{Ge}_{40-x}\text{In}_x\text{Se}_{60}$  ( $10 \leq x \leq 40$  at.%) thin films before and after annealing.

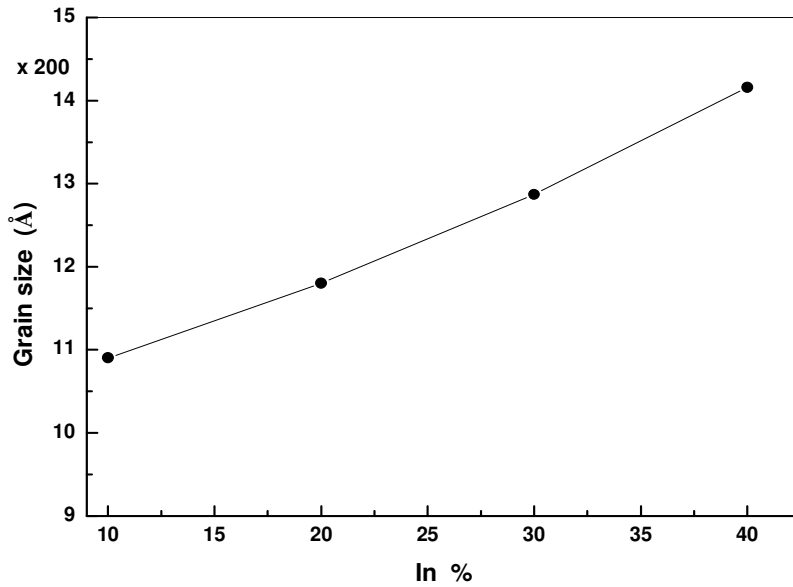


Fig. (6): Variation of grain size with In content of annealed  $\text{Ge}_{40-x}\text{In}_x\text{Se}_{60}$  ( $10 \leq x \leq 40$  at.%) thin films at 485 K for 4 hs.

#### 4. Conclusion:

The electrical conductivity results of the as-deposited  $\text{Ge}_{40-x}\text{In}_x\text{Se}_{60}$  ( $10 \leq x \leq 40$  at.%) thin films show two types of conduction mechanisms. The first mechanism due to hopping is applicable from 300-333 K while the free carrier describes the conductivity in the temperature range from 333-430 K. The results show that the conductivity of annealed films is higher than that of the as-deposited films. Accordingly, the activation energy of annealed films is lower than that of the as-deposited films. Increasing the In content in the investigated films increases the measured conductivity. The grain size is increased with increasing the In content. The increased grain size is attributed to a phase transformation from  $\text{In}_2\text{Se}_3$  to  $\text{In}_6\text{Se}_7$  phase. The increase in the coordination number of the investigated samples with increasing In-content leads to a decrease in the band gap value, which in turn increases the electrical conductivity of the annealed GeInSe films.

**References:**

1. V. Kolobov, J. Tominaya, J. Optoelectron. *Adv. Mater.* **4**, 679 (2002).
2. T. Ohta, J. Optoelectron. *Adv. Mater.* **3**, 609 (2001).
3. I. D. Aggarwal, J. S. Sanghera, J. Optoelectron. *Adv. Mater.* **4**, 665 (2002).
4. M. Lain, A. B. Seddon, *J. Non-Cryst. Solids* **184**, 30 (1995).
5. A. B. Seddon, *J. Non-Cryst. Solids* **184**, 44 (1995).
6. S. A. Khan, M. Zulfequar, M. Husain, *Physica B* **324**, 336 (2002).
7. Z. U. Borisova, "*Glassy Semiconductors*", Plenum Press, New York, p. 20 (1981).
8. N. F. Mott, *Philos. Mag.* **19**, 835 (1969).
9. M. I. Mitkova, *Mat. Chem. and Phys.* **26**, 139 (1990).
10. A. Kumar, M. Hussain, S. Swarup, A. N. Nigam and A. Kumar, *Physica B* **162**, 177 (1990).
11. J. M. Saiter, J. Ledru, G. Saffarini, S. Benazeth, *Materials Letters* **28**, 451 (1996).
12. M. K. Rabinal, K. S. Sangunni, E. S. R. Gopal, *J. Non-Cryst. Solids* **188** (1995) 98.
13. S. Mahadevan, A. Z. Giridhar, *J. Mater. Sci.* **29**, 3837 (1994).
14. S. Kumar, R. Aroka and A. Kumar, *J. Mater. Sci. Lett.* **10**, 1280 (1991).
15. L. Tichy and H. Ticha, *Mater. Lett.* **21**, 313 (1994).
16. A. Giridhar and S. Mahadevan, *J. Non-Cryst. Solids* **134**, 94 (1991).
17. S. Tolansky, "*Multiple-beam Interferometry of Surface and Films*", Oxford University Press, London, pp.147-150 (1988).
18. S. Asokan, G. Parthasarathy, *J. Non-cryst. Solids* **86**, 48 (1986).
19. V. Damodara Das and P. Gopal Ganesan, *Semicond. Sci. Tech.* **12**, 195 (1997).
20. H. Neumann, E. Nowak and C. Kuhn, *Crystal Res. Tech.* **16**, 1369 (1981).
21. J. Y. W. Seto, *J. Appl. Phys.* **46** 5247 (1975).
22. V. Damodara Das and S. Selvaraj, *J. Appl. Phys.* **83**, 3696 (1998).
23. Sangeeta Singh, R. S. Sharma, R. K. Shukla and A. Kumar, *Vacuum* **72**, 1 (2004).
24. M. A. Abdel-Rahim, M. M. Hafiz and A. M. Shamekh, *Physica B* **369**, 143 (2005).
25. J. C. Phillips, *J. Non-Cryst. Solids* **34**, 153 (1979).
26. J. M. Saiter, J. Ledru, G. Saffarini and S. Benazeth, *Material Letters* **35**, 309 (1998).
27. G. Saffarini, J. Matthiesen and R. Blachnik, *Physica B* **305**, 293 (2001).
28. M. A. Abdel-Rahim, A. Y. Abdel-latif, A. S. Soltan and M. Abu El-Oyoun, *Physica B* **322**, 252 (2002).
29. P. Arun and A. G. Vedeshwar, *Materials Research Bulletin* (U. S. A.), **38**, 1929 (2003).

30. V. K. Gandotra, K. V. Ferdinand, C. Jagadish, A. Kumar and P. C. Mathur, *phys. stat. sol. (a)* **98**, 595 (1986).
31. M. A. Urena, M. Fontana, B. Arcondo and M.T. Chavaguera-Mora, *J. Non-Cryst. Solids* **320**, 151 (2003).
32. G. Saffarini, A. Saiter, M. R. Garda and J. M. Saiter, *Physica B* **389**, 275 (2007).
33. A. Grandjean, M. Malki and C. Simonnet, *J. Non-Cryst. Solids* **352**, 2731-2736 (2006).